Continuously and (or) discretely tunable optical parametric oscillator

V.S. Ayrapetyan

Siberian State Geodesic Academy, Novosibirsk

Received May 26, 2008

A $LiNbO_3$ optical parametric oscillator (OPO) continuously and (or) discretely tunable in a spectral range 1.4–4.24 μm (with discrete tuning from 0 to 12 nm) has been designed. The OPO ring circuit provides output power up to 45 mJ with a bandwidth of 3.5 cm^{-1}. A Fabry–Perrot etalon introduced into the OPO narrows the bandwidth down to 0.7 cm^{-1}.

Introduction

Tunable sources of laser radiation in the near and middle IR wavelength range (1.41–4.24 μm) are of great practical interest. They can be used in spectroscopic problems of remote sensing of gas molecules. The most promising are tunable lasers on the basis of parametric light generation with the use of nonlinear crystals. As a rule, Nd pulse lasers are used as pumping sources and $LiNbO_3$, $KNbO_3$, KTP, KTA, etc. crystals – as nonlinear frequency converters.[1] Low angular divergence, along with narrow spectral width, and high output power are important characteristics of optical parametric oscillator (OPO) in remote sensing of gas molecules.

At present, many optical circuits of OPO cavity are realized.[2–7] The study of the simplest linear circuits[3,4] show that the radiation divergence of such oscillators is sufficiently high at satisfactory power parameters and strongly increases with pumping power. The use of a confocal unstable cavity of OPO provides for a high quality of the output beam with the divergence close to the diffraction. However, such cavities are especially sensitive to misadjustment and suitable only for oscillation at a fixed wavelength. Theoretical studies of optical cavities of OPO[9] and their computer simulation[10] show that image-rotation cavities provide for high quality of the output beam.

The results of our experimental study[11] and a number of works, e.g., Ref. 6, show that the triple-mirror ring circuit of OPO cavity provides for a low beam divergence at high power parameters.

The purpose of our study is the design of a high-efficiency OPO, continuously and (or) discretely tunable in a 1.41–4.24 μm wavelength range; the discrete tuning (from pulse to pulse) is adjustable from 0 to 12 nm; this is attained by means of supplying to nonlinear crystal's nonworking side surfaces of a DC voltage, the magnitude of which determines the frequency discrete step. In this work, maximal DC voltage is equal to 4500 V. This value could be changed in every 50 V, it corresponds to a minimal OPO frequency step, equal to 0.133 nm.

Thus, there is no discrete tuning in the absence of external field ($E = 0$); at an external voltage $U = 4500$ V the maximum of discrete tuning is 12 nm.

To provide for the above types of OPO frequency tuning, a nonlinear crystal of lithium niobate ($LiNbO_3$) with high nonlinear and electrooptic coefficients has been chosen. The choice of a triple-mirror ring cavity is stipulated by the advantage of this optical circuit over linear ones, because it allows realization of travel-wave parametric generation. A triple-mirror cavity is less sensitive to the misadjustment. There are no standing waves in such a cavity; radiation intensity in it is essentially more homogeneous in comparison with linear ones. The latter is of special importance, because of relatively low breakdown of $LiNbO_3$ crystal (300 MW/cm^2). In a triple-mirror cavity, the image rotation is carried out after each traversal. This essentially compensates discontinuity of the transverse structure of OPO generation beam and diminishes the influence of optical inhomogeneities of the pumping beam on the $LiNbO_3$ crystal.

1. Experiment

To pump OPO, the laser with an active YAG:Nd^{3+} element of 6.3 mm in diameter and 100 mm in length, assembled following the telescopic unstable cavity circuit, is used. Its radiation power is 160 mJ at $\lambda = 1.064$ μm, the pulse width is 10 ns. An optimal pulse rate, at which the power slightly differed from the mean power in the infrequent pulse mode, is at a level of 20–30 Hz. Note, that strong power instability (more than 30%) occurs when increasing pulse rate (> 30 Hz). The radiation is linearly polarized in a horizontal plane. The beam intensity distribution in the cross section has a shape of concentric rings.

Figure 1 shows the optical scheme of the triple-mirror ring OPO cavity. The active element of nonlinear $LiNbO_3$ crystal of 10×10×30 mm in size has the following orientation: $\theta = 47°$, $\varphi = -90°$.

0235-6880/08/10 791-04 $02.00

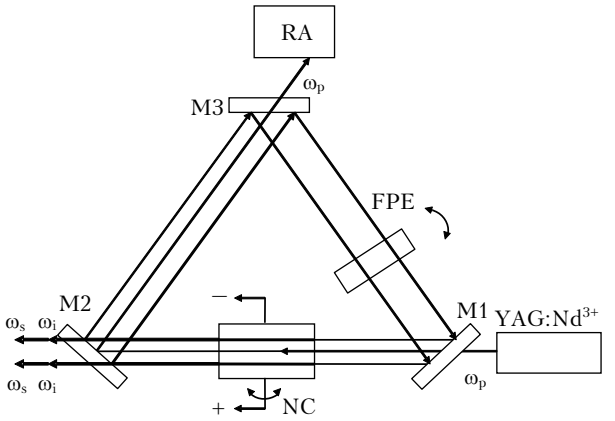

Fig. 1. Optical scheme of the ring OPO cavity: YAG:Nd^{3+} pumping laser; NC is the nonlinear $LiNbO_3$ crystal; M1, M2, and M3 are mirrors; FPE is the Fabry – Perot etalon; RA is the pumping laser radiation absorber; ω_s, ω_i, and ω_p are the signal and idler frequencies, and the frequency of pumping laser.

The diameter of the pumping beam at the crystal input is 6 mm. The nonlinear crystal is mounted on a rotating platform with a step motor (SM), having a rotating accuracy of 3 arcsec and step size of 0.03 cm^{-1}. Rotation of the nonlinear crystal about its vertical axis provides for continuous tuning of OPO output radiation wavelength. The SM is controlled by a specially written MATLAB-6 program, the SM step size corresponds to the spectral width of OPO radiation. At a corresponding setting of the PC interface, the spectral range of OPO radiation is scanned. The scanning time of the whole spectral range of OPO tuning (1.41–1.85, 2.9–4.2 μm) is 5.2 s, the step size of continuous tuning corresponds to the spectral width of OPO radiation (0.7 cm^{-1}).

The shift of the OPO radiation wavelength due to crystal temperature heating is computer-controlled and compensated with an error of 0.1°C. An additional converging of the spectral width of OPO radiation is attained by introducing the Fabry – Perot etalon (FPE) into the OPO cavity, which is also mounted on the rotating platform. FPE acts immediately on the signal wave, automatically converging the idler wave as well. Tuning of FPE passband to a necessary spectral line is performed by means of angular rotation of its axis relative to the direction of the incident radiation. FPE is mounted at those part of OPO cavity, where the high-power radiation of the pumping wave is absent. Thus, the most favorable conditions for its proper work are provided.

Figure 2 shows the optical scheme for measuring wavelength and OPO radiation spectrum width.

For this purpose, a part of OPO (*2*) output radiation, reflecting from the plane-parallel CaF_2 plate (*3*), is directed to calibration and wavelength tuning module (*8*), which is a diffusive scattering sphere with two identical PbSe photoreceivers FP-219 (*5*). One of the photoreceivers is used for mathematical subtraction of power instabilities.

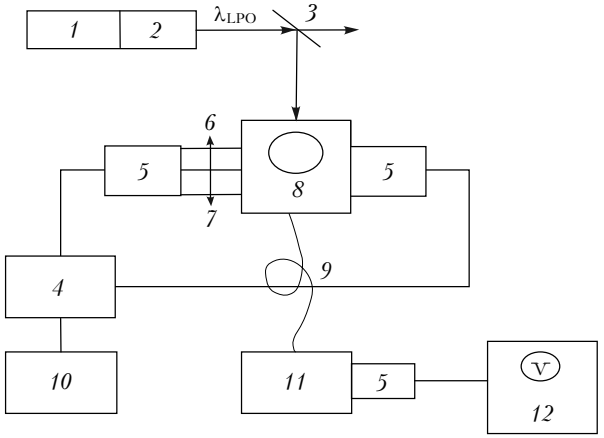

Fig. 2. Optical scheme for measuring wavelength and OPO radiation spectrum width: pumping YAG:Nd^{3+} laser (*1*); OPO module (*2*); plane-parallel CaF_2 plate (*3*); analog-to-digital converter (ADC) (*4*); PbSe photoreceiver FP-219 with preamplifier (*5*); cell with methane (*6*); cell with gas (*7*); diffusive scattering sphere (*8*); CaF_2 IR light guide fiber (*9*); PC (*10*); monochromator MDR-12 (*11*); oscillograph C1-91 (*12*).

The radiation with a known gas (in our case, methane of 90% in purity at 1-atm pressure) falls through cell (*6*) or (*7*) onto another photoreceiver. Then, electric signals from the photoreceivers come to two inputs of ADC (*4*), the output of which is connected with PC (*10*). The rovibrational absorption spectrum υ_3 of the methane band, the central *Q*-branch of which is the reference line, is displayed on the PC's monitor screen. To calibrate OPO wavelength, there is a possibility to mount IR light guide fiber GF-F-160 (*9*) on the scattering sphere, through which the laser radiation is fed to the entrance slit of the monochromator MDR-12 (*11*).

Such solution allows the automatic tuning of radiation wavelength to the preset one. The OPO output radiation power is measured with a calorimetric power meter S310 (USA).

2. Results and discussion

Power characteristics of OPO were measured in the ultimate temperature conditions both in laboratory (+30°C) and field (–10°C) conditions. Under these conditions, the power instability did not exceed ±6% after 30 min of laser operation with a pulse frequency of 25 Hz.

The OPO radiation power is shown in Fig. 3 as a function of lengths of the signal (λ = 1.42–1.75 μm) and idler (λ = 2.9–4.2 μm) waves.

The sharp fall of the signal wave power near 1.69 μm and the absence of generation of the idler wave near 2.85 μm are concerned with the strong absorption of lithium niobate near 2.85 μm. A total conversion factor of 25% is reached in the used OPO scheme. The value of beam angular convergence was calculated according to Ref. 9 as the ratio of the

aperture diameter, to which 86% of total pulse power of OPO radiation falls, to the lens focal length (d/l). The aperture was placed in the lens plane. Based on the known properties of a thin lens, it is fair to say that the measurement results of beam spatial parameters allow the angular distribution of laser radiation in a far zone to be found. Again, since the OPO generation is represented as a superposition of signal and idler waves, the known beam parameters in the far zone allow estimating the distribution character in individual waves. Experimentally obtained divergence values of signal and idler waves of OPO radiation did not exceed 3.5 mrad in the whole generation range (Fig. 4).

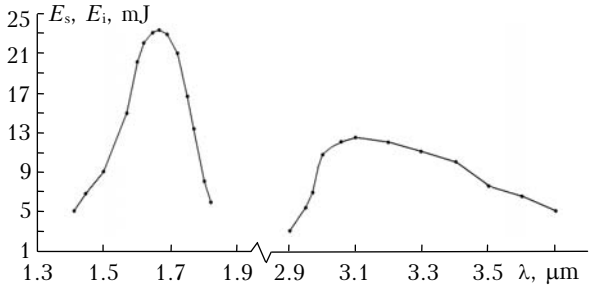

Fig. 3. Distribution of OPO radiation power in the signal and idler waves.

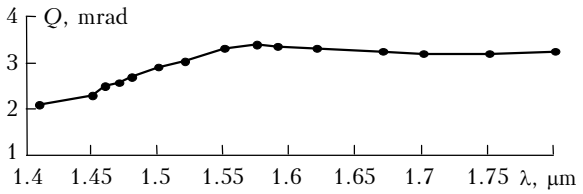

Fig. 4. OPO radiation divergence angle versus signal wavelength.

This value did not vary noticeably at a slight varying of the cavity length. The obtained result coincided with the M^2-calculated radiation divergence, which shows to what extent the beam divergence exceeds the diffraction limit.[12]

Figure 5 presents the OPO radiation spectra for an arbitrary idler wave.

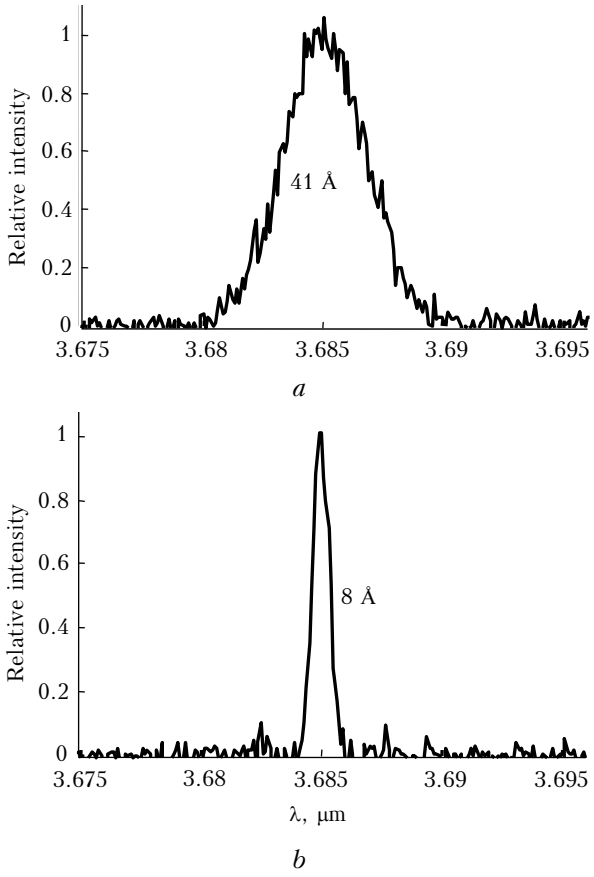

Fig. 5. OPO radiation spectrum at λ = 3.685 μm without (*a*) and with (*b*) FPE.

Figure 5*a*, corresponds to the case, when the cavity is free of FPE, while figure 5*b* shows how the OPO radiation spectrum converges in the presence of FPE. Similar spectra were obtained in the whole wavelength range of OPO tuning.

Institution	OPO specifications					
	Laser type	Wavelength, μm	Power, mJ	Spectral width of radiation, cm^{-1}	Divergence, mrad	Conversion efficiency, %
SSGA, Novosibirsk, Russia	YAG:Nd^{3+} with OPO	1.41–4.24 continuously and (or) discretely	45	0.7–0.9	3.5	25
KSU, Krasnodar, Russia	YAG:Nd^{3+} with OPO	3.7–5.7 continuously	3	–	10	4.9
B.I. Stepanov Institute of Physics, Misnk, NASB	YAG:KGW with OPO	1.54–1.61 continuously	22	5	3.5	0.4
Polyus Research and Development Institute, Moscow, Russia	YAG:Nd^{3+} with OPO	1.5–2 continuously	20	1	7	40
OPO-Lidar (USA Tatra)	YAL:Nd^{3+} with OPO	1.55–3.3 continuously	0.5–10	3.5–5	5	10
OPO-Lidar (USA Redmond)	YAG:Ti sapphire with OPO	2.2–4 continuously	Up to 30	3.5–5	5	–

Convergence of the half-width of OPO radiation spectra varied from 4 to 5 times, while OPO radiation power varied insignificantly.

Table gives some key specifications of IR OPO in comparison with analogous devices.

Thus, the continuously and (or) discretely tunable IR OPO has been designed on the base of study results of nonlinear optical properties of $LiNbO_3$ and KTP crystals and modern engineering, hardware, and software developments. Owing to its specifications, the IR OPO can be used both in lidar complexes and for solving different fundamental spectroscopic problems.

References

1. V.G. Dmitriev, G.G. Gurzadyan, and D.N. Nikogosyan, *Handbook of Nonlinear Optical Crystals* (Springer, New York, 1999), 345 pp.
2. M.D. Ewbank and M.J. Rosker, J. Opt. Soc. Am. B **14**, No. 3, 668–671 (1997).
3. A.V. Smith, W.J. Alford, T.D. Raymond, and M.S. Bowers, J. Opt. Soc. Am. B **12**, 2253–2257 (1995).
4. L.R. Marshal, A.D. Hay, and R. Burnham, Tech. Dig. Papers Adv. CLEO'90 postdeadline paper CDPO 35–1 (New York, 1990).
5. A.H. Harutjunyan, G.A. Papyan, S.S. Sargsyan, and T.K. Sargsyan, *High Efficiency Intricately Optical Parametric Oscillator based on a Litium Niobate Cristal*. ICONO'91, I, PWH12P, 167 (Leningrad, 1991).
6. V.L. Naumov, A.M. Onishchenko, A.S. Podstavkin, and A.V. Shestakov, Quant. Electron. **32**, No. 3, 225–228 (2002).
7. L.I. Vodchits, V.I. Dashkevich, N.S. Kazak, V.K. Pavlenko, V.I. Pokryshkin, I.P. Petrovich, V.V. Rukhovets, A.S. Kraskovskii, and V.A. Orlovich, Zh. Prikl. Spektrosk. **73**, No. 2, 255–259 (2006).
8. M.K. Brown and M.S. Bowers, Proc. SPIE **2986**, 113–115 (1997).
9. Yu.A. Anan'ev, *Optical Cavities and Laser Beams* (Nauka, Moscow, 1990), 211 pp.
10. A.V. Smith and M.S. Bowers, J. Opt. Soc. Am. B **18**, No. 5, 706 (2001).
11. V.S. Ayrapetyan, G.M. Apresyan, K.A. Sargsyan, and T.K. Sargsyan, *Abstract of Reports at the Conf. "LAT,"* LMI 72, Moscow (2002), pp. 89–91.
12. N. Hodgson and H. Weber, *Optical Resonator: Fundamentals, Advanced, Concepts, and Application* (Springer-Verlag, London, 1997), 226 pp.